Journal of Southeast University (English Edition) Vol. 27, No. 2, pp. 148 – 153 June 2011 ISSN 1003—7985

Construction of a complete set of similarity invariants using pseudo-Zernike moments

Gui Zhiguo[1] Zhang Hui[2] Chen Beijing[2] Shu Huazhong[2]

([1]National Key Laboratory for Electronic Measurement Technology, North University of China, Taiyuan 030051, China)
([2]Laboratory of Image Science and Technology, Southeast University, Nanjing 210096, China)

Abstract: To resolve the completeness and independence of an invariant set derived by the traditional method, a systematic method for deriving a complete set of pseudo-Zernike moment similarity (translation, scale and rotation) invariants is described. First, the relationship between pseudo-Zernike moments of the original image and those of the image having the same shape but distinct orientation and scale is established. Based on this relationship, a complete set of similarity invariants can be expressed as a linear combination of the original pseudo-Zernike moments of the same order and lower order. The problem of image reconstruction from a finite set of the pseudo-Zernike moment invariants (PZMIs) is also investigated. Experimental results show that the proposed PZMIs have better performance than complex moment invariants.

Key words: pseudo-Zernike moments; completeness; similarity invariant; image reconstruction

doi: 10.3969/j.issn.1003 – 7985.2011.02.007

Moment functions have been widely used in pattern recognition[1–2], image analysis[3–4], edge detection[5–6] and texture analysis[7]. Different types of moment functions such as geometric moments, orthogonal moments, complex moments and rotational moments are all useful tools in the field of pattern recognition and can be used to describe the image features. Among them, moments with orthogonal basis functions (e.g., Legendre, Zernike and pseudo-Zernike polynomials) can represent the image by a set of mutually independent descriptors, and thus have a minimal amount of information redundancy. Pseudo-Zernike moments (PZMs), similar to Zernike moments, possess the good properties of orthogonality and rotation invariance. Since PZMs contain $(M+1)^2$ linearly independent polynomials of order up to M, while Zernike moments have $(M+1)(M+2)/2$ linearly independent polynomials due to the additional constraints of $p-|q|$ being even, thus PZMs have better feature representation capability. It is also proven that the PZMs are more robust to image noise than the conventional Zernike moments[4].

As noted by Ghorbel et al.[8], the most important properties to be verified by the image descriptors are: 1) invariance against some geometrical transformations (translation, rotation, scaling, etc.); 2) stability to noise, to blur, to non-rigid and small local deformation; and 3) completeness. A set of invariant descriptors is said to be complete if it satisfies the following property: two objects have the same shape if and only if they have the same set of invariants[9]. In the past, the study on the completeness of moment invariants has attracted the attention of several research groups. Flusser et al.[10–11] proposed a complete set of rotation invariants by normalizing the complex moments. The construction of a complete set of similarity invariant descriptors by means of some linear combinations of complex moments was studied by Ghorbel and Derrode et al.[8, 12]. In Ref. [8], Ghorbel et al. aslo discussed the problem of image reconstruction from the complete set of moment invariants. Because the complex moments are not orthogonal, they proposed an approach to resolve the reconstruction problem by exploiting the link between the discrete Fourier transform of an image and its complex moments.

The goal of this paper is to propose a new method to achieve a complete set of similarity invariants extracted from pseudo-Zernike moments. We first establish the relationship between the pseudo-Zernike moments of the original image and those of the scaled and rotational images. Based on this relationship, the complete set of scale and rotation invariants can thus be achieved. We then investigate the image reconstruction problem using a finite set of pseudo-Zernike moment invariants (PZMIs).

1 Mathematical Background

1.1 Pseudo-Zernike moments

A two-dimensional PZM Z_{pq} of order p with repetition q of an image intensity function $f(r,\theta)$ is defined as[13]

$$Z^f_{p,q}=\frac{p+1}{\pi}\int_0^{2\pi}\int_0^1 R_{p,q}(r,\theta)\,\mathrm{e}^{-\mathrm{j}q\theta}f(r,\theta)\,r\mathrm{d}r\mathrm{d}\theta \qquad |q|\leqslant p \quad (1)$$

where $R_{p,q}(r)$ is the real-valued radial polynomial given by

$$R_{p,q}(r)=\sum_{k=0}^{p-|q|}(-1)^k\frac{(2p+1-k)!}{k!(p+|q|+1-k)!(p-|q|-k)!}r^{p-k} \quad (2)$$

1.2 A complete set of complex moment invariants

Ghorbel et al.[8] proposed a complete set of both scale and rotation invariants of complex moments given by

$$\mathrm{CMI}^f_{p,q}=\Gamma_f^{-(p+q+2)}\,\mathrm{e}^{-\mathrm{j}(p-q)\theta_f}\varphi^f_{p,q} \quad (3)$$

where $\theta_f=\arg(\varphi^f_{1,0})$, $\Gamma_f=\sqrt{\varphi^f_{0,0}}$, and $\varphi^f_{p,q}$ is a complex moment of an image function $f(r,\theta)$ defined as

Received 2011-02-02.

Biography: Gui Zhiguo(1972—), male, doctor, professor, gui_zg@163.com.

Foundation item: The National Natural Science Foundation of China (No. 61071192, 61073138).

Citation: Gui Zhiguo, Zhang Hui, Chen Beijing, et al. Construction of a complete set of similarity invariants using pseudo-Zernike moments[J]. Journal of Southeast University (English Edition), 2011, 27(2): 148 – 153. [doi: 10.3969/j.issn.1003 – 7985.2011.02.007]

$$\varphi_{p,q}^{f} = \int_0^{\infty}\int_0^{2\pi} r^{p+q+1} e^{j(p-q)\theta} f(r,\theta)\,dr d\theta \qquad p,\ q \geqslant 0 \quad (4)$$

2 Method

2.1 A complete set of similarity invariants of PZMs

Eq. (2) shows that the radial polynomial $R_{pq}(r)$ is symmetric about q, i.e., $R_{p,-q}(r) = R_{pq}(r)$ for $q \geqslant 0$. Thus, for the study of these polynomials, we can only consider the case where $q \geqslant 0$. Let $p = q + m$ with $m \geqslant 0$, Eq. (2) can be rewritten as

$$R_{q+m,q}(r) = \sum_{k=0}^{m} (-1)^{m-k} \frac{(2q+m+1+k)!}{(m-k)!(2q+1+k)!(k)!} r^{q+k} = \sum_{k=0}^{m} c_{m,k}^{q} r^{q+k} \quad (5)$$

where

$$c_{m,k}^{q} = (-1)^{m-k} \frac{(2q+m+1+k)!}{k!(m-k)!(2q+1+k)!} \quad (6)$$

Let $\boldsymbol{U}_m^q(r) = \{R_{q,q}(r), R_{q+1,q}(r), \ldots, R_{q+m,q}(r)\}^{\mathrm{T}}$ and $\boldsymbol{M}_m^q(r) = \{r^q, r^{q+1}, \ldots, r^{q+m}\}^{\mathrm{T}}$, we have

$$\boldsymbol{U}_m^q(r) = \boldsymbol{C}_m^q \boldsymbol{M}_m^q(r) \quad (7)$$

where $\boldsymbol{C}_m^q = (c_{i,j}^q)$ with $0 \leqslant j \leqslant i \leqslant m$ is an $(m+1)\times(m+1)$ lower triangular matrix whose element $c_{i,j}^q$ is given by Eq. (6). Since all the diagonal elements of $\boldsymbol{C}_m^q$ are not zero, matrix $\boldsymbol{C}_m^q$ is non-singular, thus

$$\boldsymbol{M}_m^q(r) = (\boldsymbol{C}_m^q)^{-1} \boldsymbol{U}_m^q(r) = \boldsymbol{D}_m^q \boldsymbol{U}_m^q(r) \quad (8)$$

where $\boldsymbol{D}_m^q = (d_{i,j}^q)$ is the inverse matrix of $\boldsymbol{C}_m^q$. It is also an $(m+1)\times(m+1)$ lower triangular matrix. The computation of the elements of $\boldsymbol{D}_m^q$ is described in the following proposition.

Proposition 1 For the lower triangular matrix $\boldsymbol{C}_m^q$, the elements of its inverse matrix $\boldsymbol{D}_m^q$ are given as

$$d_{i,j}^q = \frac{(2q+2j+2)\,i!\,(2q+i+1)!}{(i-j)!(2q+i+j+2)!} \quad (9)$$

Proof To prove the proposition, we need to demonstrate the following equation,

$$\sum_{s=l}^{k} c_{k,s}^q d_{s,l}^q = \delta_{k,l} \quad (10)$$

For $k = l$, we have

$$c_{k,k}^q d_{k,k}^q = 1 \quad (11)$$

For $l < k$, we have

$$\sum_{s=l}^{k} c_{k,s}^q d_{s,l}^q = \sum_{s=l}^{k} (-1)^{k-s} \frac{(2q+k+1+s)!(2q+2l+2)}{(k-s)!(s-l)!(2q+s+l+2)!} = (-1)^k (2q+2l+2) \sum_{s=l}^{k} F(q,k,l,s) \quad (12)$$

where

$$F(q,k,l,s) = \frac{(-1)^s (2q+k+1+s)!}{(k-s)!(s-l)!(2q+s+l+2)!} \quad (13)$$

Let

$$G(q,k,l,s) = \frac{(-1)^{s+1}(2q+k+1+s)!}{(k+1-s)!(s-l)!(2q+s+l+1)!} \cdot \frac{(k+1-s)(s-l)}{(k-l)(2q+k+l+2)} \quad (14)$$

It can then be easily verified that

$$F(q,k,l,s) = G(q,k,l,s+1) - G(q,k,l,s) \quad (15)$$

Thus

$$\sum_{s=l}^{k} F(q,k,l,s) = \sum_{s=l}^{k} [G(q,k,l,s+1) - G(q,k,l,s)] = G(q,k,l,k+1) - G(q,k,l,l) = 0$$

We deduce from Eq. (12) that

$$\sum_{s=l}^{k} c_{k,s}^q d_{s,l}^q = 0 \qquad l < k \quad (16)$$

The proof is now complete.

Note that the proof of Proposition 1 is inspired by a technique proposed by Petkovsek et al [14].

We now consider that the two images f and g have the same shape but distinct orientation β and scale α; i.e., $g(r,\theta) = f(r/\alpha, \theta-\beta)$ and the pseudo-Zernike moment of the image intensity function $g(r,\theta)$ is defined as

$$Z_{q+m,q}^{g} = \frac{q+m+1}{\pi}\int_0^{2\pi}\int_0^1 R_{q+m,q}(r)\,e^{-jq\theta} g(r,\theta)\,r dr d\theta = \alpha^2 e^{-jq\beta}\frac{q+m+1}{\pi}\int_0^{2\pi}\int_0^1 R_{q+m,q}(\alpha r)\,e^{-jq\theta} f(r,\theta)\,r dr d\theta \quad (17)$$

Let $\boldsymbol{U}_m^q(\alpha r) = \{R_{q,q}(\alpha r), R_{q+1,q}(\alpha r), \ldots, R_{q+m,q}(\alpha r)\}^{\mathrm{T}}$ and $\boldsymbol{M}_m^q(\alpha r) = \{(\alpha r)^q, (\alpha r)^{q+1}, \ldots, (\alpha r)^{q+m}\}^{\mathrm{T}}$. It can be easily deduced from Eq. (7) that

$$\boldsymbol{U}_m^q(\alpha r) = \boldsymbol{C}_m^q \boldsymbol{M}_m^q(\alpha r) \quad (18)$$

Otherwise,

$$\boldsymbol{M}_m^q(\alpha r) = \mathrm{diag}(\alpha^q, \alpha^{q+1}, \ldots, \alpha^{q+m})(r^q, r^{q+1}, \ldots, r^{q+m})^{\mathrm{T}} = \mathrm{diag}(\alpha^q, \alpha^{q+1}, \ldots, \alpha^{q+m})\boldsymbol{M}_{\mathrm{m}}^{\mathrm{q}}(r) \quad (19)$$

Substituting Eqs. (19) and (8) into Eq. (18), we obtain

$$\boldsymbol{U}_m^q(\alpha r) = \boldsymbol{C}_m^q \mathrm{diag}(\alpha^q, \alpha^{q+1}, \ldots, \alpha^{q+m}) \boldsymbol{D}_m^q \boldsymbol{U}_m^q(r) \quad (20)$$

By expanding Eq. (20), we obtain

$$R_{q+m,q}(\alpha r) = \sum_{k=0}^{m} R_{q+k,q}(r) \sum_{l=k}^{m} \alpha^{q+l} c_{m,l}^q d_{l,k}^q \quad (21)$$

By Eq. (21), Eq. (17) can be rewritten as

$$Z_{q+m,q}^{g} = \alpha^2 e^{-jq\beta}\frac{q+m+1}{\pi} \cdot \int_0^{2\pi}\int_0^1 \Big(\sum_{k=0}^{m} R_{q+k,q}(r) \sum_{l=k}^{m} \alpha^{q+l} c_{m,l}^q d_{l,k}^q\Big) e^{-jq\theta} f(r,\theta)\,r dr d\theta = e^{-jq\beta} \sum_{k=0}^{m} \frac{q+m+1}{q+k+1}\Big(\sum_{l=k}^{m} \alpha^{q+l+2} c_{m,l}^q d_{l,k}^q\Big) Z_{q+k,q}^{f} \quad (22)$$

Eq. (22) shows that the 2D scaled and rotational PZMs, $Z_{q+m,q}^{g}$, can be expressed as a linear combination of the orig-

inal PZMs $Z^f_{q+k,\,q}$ with $0 \leqslant k \leqslant m$. Based on this relationship, we can construct a complete set of both rotation and scale invariants $\mathrm{PZMI}^f_{q+m,\,q}$ which is described in the following theorem.

Theorem 1 For a given integer q and any positive integer m, let

$$\mathrm{PZMI}^f_{q+m,\,q} = \sum_{k=0}^{m} \mathrm{e}^{-\mathrm{j}q\theta_f} \frac{q+m+1}{q+k+1} \Big(\sum_{l=k}^{m} \Gamma_f^{-(q+l+2)} c^q_{m,\,l}\, d^q_{l,\,k} \Big) Z^f_{q+k,\,q} \tag{23}$$

with $\theta_f = \arg(Z^f_{1,\,1})$ and $\Gamma_f = \sqrt{Z^f_{0,\,0}}$. Then $\mathrm{PZMI}^f_{q+m,\,q}$ is invariant to both image rotation and scaling.

Proof Eq. (23) can be rewritten in a matrix form as

$$\begin{bmatrix} \mathrm{PZMI}^f_{q,\,q} \\ \mathrm{PZMI}^f_{q+1,\,q} \\ \vdots \\ \mathrm{PZMI}^f_{q+m,\,q} \end{bmatrix} = \mathrm{e}^{-\mathrm{j}q\theta_f} \mathrm{diag}(q+1,\, q+2,\, \ldots,\, q+m+1) \cdot \boldsymbol{C}^q_m \mathrm{diag}(\Gamma_f^{-(q+2)},\, \Gamma_f^{-(q+3)},\, \ldots,\, \Gamma_f^{-(q+m+2)}) \cdot \boldsymbol{D}^q_m \mathrm{diag}\Big(\frac{1}{q+1}, \frac{1}{q+2}, \ldots, \frac{1}{q+m+1}\Big) \begin{bmatrix} Z^f_{q,\,q} \\ Z^f_{q+1,\,q} \\ \vdots \\ Z^f_{q+m,\,q} \end{bmatrix} \tag{24}$$

Eq. (22) can be rewritten in a matrix form as

$$\begin{bmatrix} Z^g_{q,\,q} \\ Z^g_{q+1,\,q} \\ \vdots \\ Z^g_{q+m,\,q} \end{bmatrix} = \mathrm{e}^{-\mathrm{j}q\beta} \mathrm{diag}(q+1,\, q+2,\, \ldots,\, q+m+1) \cdot \boldsymbol{C}^q_m \mathrm{diag}(\alpha^{q+2},\, \alpha^{q+3},\, \ldots,\, \alpha^{q+m+2}) \boldsymbol{D}^q_m \cdot \mathrm{diag}\Big(\frac{1}{q+1}, \frac{1}{q+2}, \ldots, \frac{1}{q+m+1}\Big) \begin{bmatrix} Z^f_{q,\,q} \\ Z^f_{q+1,\,q} \\ \vdots \\ Z^f_{q+m,\,q} \end{bmatrix} \tag{25}$$

In particular, we have

$$\left.\begin{aligned} \Gamma_g &= \alpha \Gamma_f,\ Z^g_{1,\,1} = \alpha^3 \mathrm{e}^{-\mathrm{j}\beta} Z^f_{1,\,1} \\ \theta_g &= \arg(Z^g_{1,\,1}) = \arg(\lambda^3 \mathrm{e}^{-\mathrm{j}\beta} \mathrm{e}^{\mathrm{j}\theta_f}) = \theta_f - \beta \end{aligned}\right\} \tag{26}$$

Substituting Eqs. (25) and (26) into Eq. (24) and using the identity $\boldsymbol{D}^q_m \boldsymbol{C}^q_m = \boldsymbol{I}$ ($\boldsymbol{I}$ is an identity matrix), we obtain

$$\begin{bmatrix} \mathrm{PZMI}^g_{q,\,q} \\ \mathrm{PZMI}^g_{q+2,\,q} \\ \vdots \\ \mathrm{PZMI}^g_{q+2m,\,q} \end{bmatrix} = \mathrm{e}^{-\mathrm{j}q\theta_f} \mathrm{e}^{\mathrm{j}q\beta} \mathrm{diag}(q+1,\, q+2,\, \ldots,\, q+m+1) \boldsymbol{C}^q_m \cdot \mathrm{diag}(\Gamma_f^{-(q+2)},\, \Gamma_f^{-(q+3)/2},\, \ldots,\, \Gamma_f^{-(q+m+2)/2}) \cdot \mathrm{diag}(\alpha^{-(q+2)},\, \alpha^{-(q+3)},\, \ldots,\, \alpha^{-(q+m+2)}) \cdot \boldsymbol{D}^q_m \mathrm{diag}\Big(\frac{1}{q+1}, \frac{1}{q+2}, \ldots, \frac{1}{q+m+1}\Big) \mathrm{e}^{-\mathrm{j}q\beta} \cdot \mathrm{diag}(q+1,\, q+2,\, \ldots,\, q+m+1) \boldsymbol{C}^q_m \cdot \mathrm{diag}(\alpha^{q+2},\, \alpha^{q+3},\, \ldots,\, \alpha^{q+m+2}) \boldsymbol{D}^q_m \cdot \mathrm{diag}\Big(\frac{1}{q+1}, \frac{1}{q+2}, \ldots, \frac{1}{q+m+1}\Big) \begin{bmatrix} Z^f_{q,\,q} \\ Z^f_{q+1,\,q} \\ \vdots \\ Z^f_{q+m,\,q} \end{bmatrix} =$$

$$\mathrm{e}^{-\mathrm{j}q\theta_f} \mathrm{diag}(q+1,\, q+2,\, \ldots,\, q+m+1) \boldsymbol{C}^q_m \cdot \mathrm{diag}(\Gamma_f^{-(q+2)},\, \Gamma_f^{-(q+3)},\, \ldots,\, \Gamma_f^{-(q+m+2)}) \cdot \mathrm{diag}\Big(\frac{1}{q+1}, \frac{1}{q+2}, \ldots, \frac{1}{q+m+1}\Big) D^q_m \begin{bmatrix} Z^f_{q,\,q} \\ Z^f_{q+1,\,q} \\ \vdots \\ Z^f_{q+m,\,q} \end{bmatrix} = \begin{bmatrix} \mathrm{PZMI}^f_{q,\,q} \\ \mathrm{PZMI}^f_{q+1,\,q} \\ \vdots \\ \mathrm{PZMI}^f_{q+1m,\,q} \end{bmatrix} \tag{27}$$

Thus, we have

$$\mathrm{PZMI}^g_{q+m,\,q} = \mathrm{PZMI}^f_{q+m,\,q} \tag{28}$$

The proof is now complete.

Using the same method to achieve the translation invariance as described in Ref. [8], the origin of the coordinate system is taken at the center of mass of the object.

It is easy to verify that the set of invariants is complete by rewriting Eq. (24) as

$$\begin{bmatrix} Z^f_{q,\,q} \\ Z^f_{q+1,\,q} \\ \vdots \\ Z^f_{q+m,\,q} \end{bmatrix} = \mathrm{e}^{\mathrm{j}q\theta_f} \mathrm{diag}(q+1,\, q+2,\, \ldots,\, q+m+1) \boldsymbol{C}^q_m \cdot \mathrm{diag}(Z^{f\ (q+2)/2}_{0,\,0},\, Z^{f\ (q+3)/2}_{0,\,0},\, \ldots,\, Z^{f\ (q+m+2)/2}_{0,\,0}) \boldsymbol{D}^q_m \cdot \mathrm{diag}\Big(\frac{1}{q+1}, \frac{1}{q+2}, \ldots, \frac{1}{q+m+1}\Big) \begin{bmatrix} \mathrm{PZMI}^f_{q,\,q} \\ \mathrm{PZMI}^f_{q+1,\,q} \\ \vdots \\ \mathrm{PZMI}^f_{q+m,\,q} \end{bmatrix} \tag{29}$$

Thus, we have

$$Z^f_{q+m,\,q} = \sum_{k=0}^{m} \mathrm{e}^{\mathrm{j}q\theta_f} \frac{q+m+1}{q+k+1} \Big(\sum_{l=k}^{m} \Gamma_f^{(q+l+2)} c^q_{m,\,l}\, d^q_{l,\,k} \Big) \mathrm{PZMI}^f_{q+k,\,q} \tag{30}$$

Eq. (30) shows that the set of invariants is complete.

2.2 Image reconstruction

Using the orthogonality property of PZMs, the image intensity function $f(r,\ \theta)$ can be reconstructed from a finite number M of PZMs as

$$\tilde{f}(r,\, \theta) = \sum_{p=0}^{M} \sum_{q} Z^f_{pq}\, V_{pq}(r,\, \theta) = \sum_{p=0}^{M} \sum_{q} Z^f_{pq}\, R_{pq}(r)\, \mathrm{e}^{\mathrm{j}q\theta} \tag{31}$$

Substituting Eq. (30) into Eq. (31) yields

$$\tilde{f}(r,\, \theta) = \sum_{p=0}^{M} \sum_{q} R_{pq}(r)\, \mathrm{e}^{\mathrm{j}q(\theta+\theta_f)} \sum_{k=0}^{p-q} \frac{p+1}{q+k+1} \cdot \Big(\sum_{l=k}^{p-q} \Gamma_f^{(q+l+2)} c^q_{p-q,\,l}\, d^q_{l,\,k} \Big) \mathrm{PZMI}^f_{q+k,\,q} \tag{32}$$

Eq. (32) shows that the original image $f(r,\ \theta)$ can be reconstructed from the complete set of PZMIs.

3 Experimental Results

In this section, several experiments are carried out to

evaluate the complete family of similarity invariants introduced in this paper using a set of gray-level images. The proposed PZMIs are compared with the complete set of complex moment invariants (CMIs) presented in Ref. [8]. For the experiments presented in this section, a set of eight images (see Fig. 1) with a size of 128×128 is chosen from the public Columbia Object Image Library (COIL-100) database[15]. In order to contain the entire transformed image after transformation, the actual size of all the original images is 204×204 by adding some background pixels.

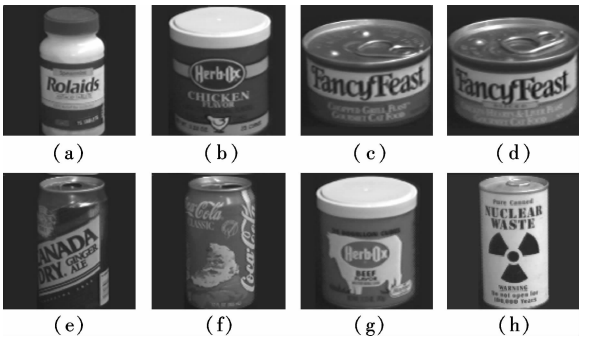

Fig. 1 Eight objects selected from the COIL-100 database

Let p be the maximum order of CMIs, and let $\boldsymbol{\psi}^f_{\mathrm{CMI}}(p) = (\mathrm{CMI}^f_{1,0}, \mathrm{CMI}^f_{0,1}, \ldots, \mathrm{CMI}^f_{p,0}, \ldots, \mathrm{CMI}^f_{0,p})$. The dimension of $\boldsymbol{\psi}^f_{\mathrm{CMI}}(p)$ is $(p+1)(p+2)/2 - 1$. For comparison purpose, we also define the vector $\boldsymbol{\psi}^f_{\mathrm{PZMI}}(p) = (\mathrm{PZMI}^f_{1,0}, \mathrm{PZMI}^f_{1,1}, \ldots, \mathrm{PZMI}^f_{p,0}, \ldots, \mathrm{PZMI}^f_{p,p})$ for the proposed PZMIs. The size of $\boldsymbol{\psi}^f_{\mathrm{PZMI}}(p)$ is also $(p+1)(p+2)/2 - 1$. The relative error between the two sets of moment invariants corresponding to an image $f(x, y)$ and its transformed image $g(x, y)$ is defined as

$$E_p(f, g) = \frac{\| \boldsymbol{\psi}^f(p) - \boldsymbol{\psi}^g(p) \|}{\| \boldsymbol{\psi}^f(p) \|} \tag{33}$$

where $\| \cdot \|$ is the Euclidean norm.

3.1 Test of invariance

To test invariance with respect to rotation, eight images shown in Fig. 1 were rotated by angles from 0° to 90° with intervals of 5°, and a bilinear interpolation was used when required. The proposed PZMIs defined in Eq. (23) and CMIs given in Eq. (3) of order up to $p = 5$ were computed for all 152 images. Fig. 2(a) shows the mean relative errors of $E_p(f_i, g_i)$, where $f_i (i = 1, 2, \ldots, 8)$ denotes the eight images shown in Fig. 1; g_i is its rotated image. It can be seen from Fig. 2(a) that the relative error of PZMIs is lower than that of the CMIs, whatever the rotational angle. We then evaluate the invariance of PZMIs with respect to image scaling. Eight images are scaled by a factor from 0.1 to 2 with intervals of 0.1, forming a set of 160 images. The mean relative errors of PZMIs and CMIs are depicted in Fig. 2(b). It is clear that the proposed PZMIs show better performance than the CMIs. To test the robustness of the invariant family against noise, we added to the same eight images a white Gaussian noise with mean $\mu = 0$ and standard deviations varying from 0 to 50 and a salt-and-pepper noise with noise density from 0 to 35%, respectively. It can be observed from Fig. 3 that, the relative error increases with the increase in the noise level; however, PZMIs are more robust to noise than CMIs.

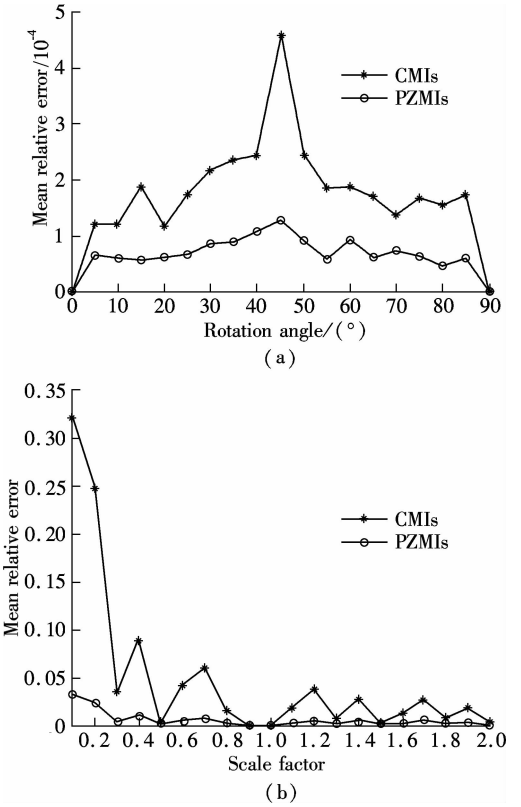

Fig. 2 Performance of the invariants to rotation and scaling. (a) Ratation with different angles; (b) Scaling with different scale factors

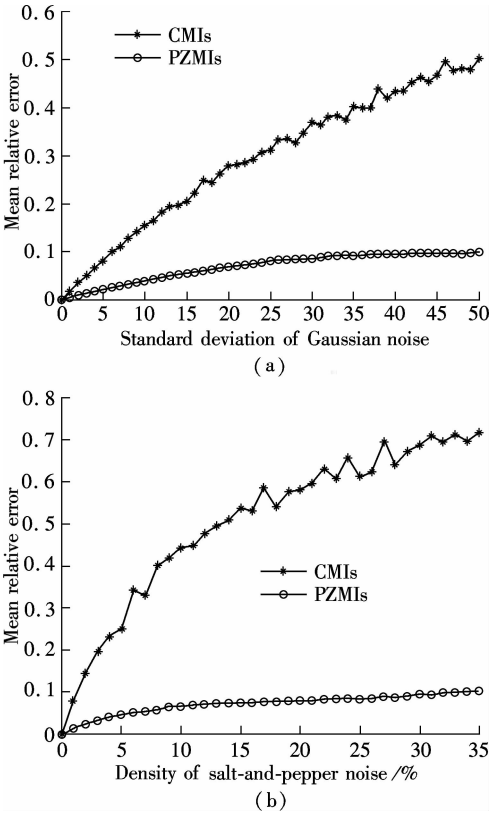

Fig. 3 Performance of the invariants with respect to noise. (a) Gaussian noise with different standard deviations; (b) Salt-and-pepper noise with different densities

3.2 Object classification

To further assess the performance of PZMIs and their robustness against noise, an object classification procedure was conducted. We also used the eight images shown in Fig. 1 as the training set. To obtain the testing set, each image was rotated at angle $\alpha \in \{0°, 30°, \ldots, 300°, 330°\}$, and scaled with scaling factor $\lambda \in \{0.5, 0.75, \ldots, 1.75, 2.0\}$, forming a set of 672 images. This was followed by adding a white Gaussian noise with different standard deviations and a salt-and-pepper noise with different noise densities. The minimum-Lance-Williams-distance classification is used as the classification method. The Lance-Williams distance between the two images f and g is defined by their moment invariant sets $\boldsymbol{\psi}^f$ and $\boldsymbol{\psi}^g$ as

$$d(f, g) = \frac{1}{n}\sum_{k=1}^{n}\frac{|\boldsymbol{\psi}_k^f - \boldsymbol{\psi}_k^g|}{|\boldsymbol{\psi}_k^f| + |\boldsymbol{\psi}_k^g|} \tag{34}$$

where $\boldsymbol{\psi}_k^f$ and $\boldsymbol{\psi}_k^g (k = 1, 2, \ldots, n)$ denote the invariants, n is the total number of invariants used in the experiment and $|\cdot|$ the magnitude of the complex number.

The classification rates using different moment invariants of order up to 5 are summarized in Tab. 1. It can be observed that: 1) The classification results are quite good (100%) for both methods in the case of noise-free; 2) The classification rates decrease with the increase in the noise level. However, the proposed PZMIs perform much better than the CMIs whatever the noise and the noise level. Although some images are highly corrupted, the classification rates of PZMIs are still higher than 86%. But this is not the case for CMIs. The reason is that the orthogonal PZMIs are more robust to noise than the non-orthogonal CMIs[4].

Tab. 1 Classification rates of CMIs and the proposed PZMIs in object classification %

Moment invariants	CMIs	PZMIs
Noise-free	100.00	100.00
Gaussian noise with STD of 10	95.09	98.81
Gaussian noise with STD of 20	84.97	94.64
Gaussian noise with STD of 30	66.07	87.65
Salt-and-pepper noise with noise density of 1%	87.05	93.30
Salt-and-pepper noise with noise density of 2%	80.95	90.77
Salt-and-pepper noise with noise density of 3%	72.47	86.76
Average rate	83.80	93.13

3.3 Image reconstruction

In this subsection, the first gray image in Fig. 1 with a size of 128×128 is used. The sequence of reconstructed images using Eq. (34) with different values of M (maximum order moment invariants used in the reconstruction) is listed in Fig. 4. Let $f(x, y)$ be the original image and $\tilde{f}(x, y)$ be the reconstructed image. The following normalized mean square error is used to measure the accuracy of the reconstructed images.

$$\varepsilon^2 = \frac{\sum_x \sum_y [\tilde{f}(x, y) - f(x, y)]^2}{\sum_x \sum_y f(x, y)^2}$$

The reconstruction errors are also given in Fig. 4. It is shown that good results can be obtained as the order of moment invariants increases, especially for $M \geqslant 60$.

Fig. 4 Image reconstruction of Fig. 1(a) with different M. (a) $M = 20$, $\varepsilon^2 = 0.030\,4$; (b) $M = 40$, $\varepsilon^2 = 0.021\,5$; (c) $M = 60$, $\varepsilon^2 = 0.019\,0$; (d) $M = 80$, $\varepsilon^2 = 0.018\,6$; (e) $M = 100$, $\varepsilon^2 = 0.018\,5$

4 Conclusion

In this paper, we present a novel method to derive a complete set of PZMIs. These PZMIs can be expressed as a linear combination of the original PZMs. The image reconstruction from a finite set of complete similarity invariant sets has been also investigated. The simulation results demonstrate the invariance properties and discriminative capabilities of the proposed descriptors.

References

[1] Hu M K. Visual pattern recognition by moment invariants [J]. *IRE Trans Inf Theory*, 1962, **8**: 179 - 187.
[2] Flusser J, Suk T. Pattern recognition by affine moment invariants [J]. *Pattern Recognit*, 1993, **26**(1): 167 - 174.
[3] Teague M. Image analysis via the general theory of moments [J]. *J Opt Soc Am*, 1980, **70**(8): 920 - 930.
[4] Teh C H, Chin R T. On image analysis by the method of moments [J]. *IEEE Trans Pattern Anal Mach Intel*, 1988, **10**(4): 496 - 513.
[5] Luo L M, Hamitouche C, Dilleseger J L, et al. A moment-based three-dimensional edge operator [J]. *IEEE Trans Biomed Eng*, 1993, **40**(7): 693 - 703.
[6] Luo L M, Xie X H, Bao X D. A modified moment-based edge operator for rectangular pixel image [J]. *IEEE Trans Circuits Systems Video Technol*, 1994, **4**(6): 552 - 554.
[7] Tuceryan M. Moment-based texture segmentation [J]. *Pattern Recognit Lett*, 1994, **15**(7): 115 - 123.
[8] Ghorbel F, Derrode S, Mezhoud R, et al. Image reconstruction from a complete set of similarity invariants extracted from complex moments [J]. *Pattern Recognit Lett*, 2006, **27**(12): 1361 - 1369.
[9] Crimmins T R. A complete set of Fourier descriptors for two dimensional shape [J]. *IEEE Trans Syst Man Cybernet*, 1982, **121**(6): 848 - 855.
[10] Flusser J. On the independence of rotation moment invariants [J]. *Pattern Recognit*, 2000, **33**(9): 1405 - 1410.
[11] Flusser J. On the inverse problem of rotation moment invariants [J]. *Pattern Recognit*, 2002, **35**(12): 3015 - 3017.
[12] Derrode S, Mezhoud R, Ghorbel F. Comparison between two complete sets of shape descriptors for 2D gray-level object content based retrieval [J]. *Ann Telecommun*, 2000, **55** (3/4): 184 - 193. (in French)
[13] Mukundan R, Ramakrishnan K R. *Moment functions in image analysis — theory and applications* [M]. Singapore: World Scientific, 1998: 60 - 60.
[14] Petkovsek M, Wilf H S, Zeilberger D. $A = B$ [M]. Wellesley, Massachusetts: AK Peters, Ltd, 1996.
[15] Nene S A, Nayar S K, Murase H. Columbia University Image Library (COIL-100) [EB/OL]. (2007-08-30) [2011-01-03]. http://www1.cs.columbia.edu/CAVE/software/softlib/coil-100.php.

完备伪 Zernike 矩相似不变量集的构造

桂志国[1] 张 辉[2] 陈北京[2] 舒华忠[2]

([1] 中北大学电子测试技术国家重点实验室,太原 030051)
([2] 东南大学影像科学与技术实验室,南京 210096)

摘要:为了解决传统方法构造的矩不变量特征集存在的完备性和独立性问题,提出了一种完备的伪 Zernike 矩相似变换(旋转、平移和缩放)不变量集的构造方法,并给出了系统的推导和证明. 首先推导了几何变换前后图像的伪 Zernike 矩之间的关系,然后基于该关系得到了伪 Zernike 矩的相似不变量集,并将其表示成变换前图像的同阶和低阶伪 Zernike 矩的线性组合. 同时,研究了通过一组有限的伪 Zernike 矩不变量进行图像重构的问题. 实验结果表明,提出的伪 Zernike 矩完备不变量集优于复数矩完备不变量集.

关键词:伪 Zernike 矩;完备性;相似不变量;图像重构

中图分类号:TP391